Published by :
https://www.ijert.org/
An International Peer-Reviewed Journal

International Journal of Engineering Research & Technology (IJERT)
ISSN: 2278-0181
Vol. 14 Issue 12 , December - 2025

CFD Analysis and Comparison of Supersonic Aircraft Nose Cone Designs for Drag Reduction

Mrs. Lukkani Sushma
Associate Professor, Department of Aeronautical Engineering
Malla Reddy College of Engineering & Technology (MRCET), Hyderabad, India.

Kanthala Saidhar, Kamarajugadda Dinesh Kumar, Paladi Sai Balaji, Harshitha Joshi
Student, Department of Aeronautical Engineering,
Malla Reddy College of Engineering & Technology (MRCET), Hyderabad, India.

***Abstract* - This study investigates the aerodynamic performance of different nose cone designs for supersonic aircraft applications using Computational Fluid Dynamics (CFD). Three nose cone geometries—conical, tangent ogive, and parabolic—were analyzed at Mach 3 across four fineness ratios (L/D = 1.5, 2.5, 3.5, 4.5) using ANSYS Fluent software. A mesh independence study confirmed solution accuracy with drag force variation below 0.01% upon refinement. The results show that increasing fineness ratio reduces drag significantly for all shapes, with the conical nose achieving the lowest drag coefficient (Cd = 0.251) at L/D=4.5. The parabolic shape performed best at moderate lengths (L/D=2.5, Cd=0.361). The study concludes that while nose cone shape is important, the fineness ratio is a critical parameter for drag optimization in supersonic flight. These findings provide practical insights for aircraft designers seeking to minimize aerodynamic resistance in high-speed applications.**

Keywords - **Computational Fluid Dynamics, Supersonic Aerodynamics, Nose Cone Design, Drag Reduction, Fineness Ratio, ANSYS Fluent**

Nomenclature

- A = *Reference frontal area [m²]*
- C_d = *Drag coefficient [-]*
- C_p = *Pressure coefficient [-]*
- D = *Base diameter of nose cone [m]; also Drag force [N]*
- K = *Parabolic shape parameter [-]*
- L = *Length of nose cone [m]*
- L/D = *Fineness ratio (length-to-diameter ratio) [-]*
- M = *Mach number [-]*
- P = *Static pressure [Pa]*
- P_∞ = *Free-stream static pressure [Pa]*
- R = *Base radius of nose cone [m]*
- T = *Temperature [K]*
- V_∞ = *Free-stream velocity [m/s]*
- x = *Axial coordinate from nose tip [m]*
- y = *Radial coordinate [m]*
- α = *Angle of attack [°]*
- β = *Shock wave angle [°]*
- γ = *Ratio of specific heats for air (= 1.4) [-]*
- θ = *Cone half-angle or flow deflection angle [°]*
- ρ *(in tangent ogive)* = *Radius of circular arc [m]*

I. INTRODUCTION

The design of supersonic aircraft nose cones presents significant aerodynamic challenges due to shock wave formation at high speeds. At Mach numbers above 1, wave drag becomes the dominant component of total drag, directly affecting fuel efficiency, range, and performance [1]. Nose cone geometry plays a crucial role in determining shock wave characteristics and subsequent drag forces [2].

Three primary nose cone shapes are commonly used in aerospace applications: conical (simple straight profile), tangent ogive (circular arc profile), and parabolic (quadratic curve profile). Each shape offers different aerodynamic characteristics, manufacturing complexities, and performance trade-offs [3]. Additionally, the fineness ratio (length-to-diameter ratio, L/D) significantly influences drag, with slender designs generally producing weaker shocks [4].

Previous studies have analyzed individual nose cone shapes, but comprehensive comparisons across multiple fineness ratios at specific Mach numbers are limited. This research addresses this gap by systematically evaluating all three geometries at Mach 3 across practical L/D ratios (1.5 to 4.5).

The primary objectives of this study are: (1) to analyze aerodynamic performance of conical, tangent ogive, and parabolic nose cones at Mach 3; (2) to investigate the effect of fineness ratio on drag characteristics; and (3) to identify optimal configurations for drag minimization.

The remainder of this paper is organized as follows: Section II details the methodology, including geometric modeling, computational setup, mesh generation, and solver configuration. Section III presents and discusses the results, encompassing flow-field visualization, drag coefficient analysis, surface pressure distributions, and validation against theoretical predictions. Section IV provides the concluding remarks and summary of key findings, while Section V outlines potential directions for future research.

International Journal of Engineering Research & Technology (IJERT)
ISSN: 2278-0181
Vol. 14 Issue 12 , December - 2025

II. METHODOLOGY

A. Geometric Modeling

Three nose cone profiles were designed using SolidWorks 2022 software, each with a constant base diameter of 1.1 m (frontal area = 0.950 m²). The mathematical definitions are:

- Conical: $y(x) = \frac{R}{L} \cdot x$
- Tangent Ogive: Circular arc with radius $\rho = \frac{L^2+R^2}{2R}$
- Parabolic (K'=1): $y(x) = R \cdot (\frac{x}{L})^{1/2}$

Where: x = axial distance from tip, y = local radius, R = base radius (0.55 m), L = nose length.
For each geometry, four models were created with lengths corresponding to L/D ratios of 1.5, 2.5, 3.5, and 4.5, resulting in 12 configurations for analysis.

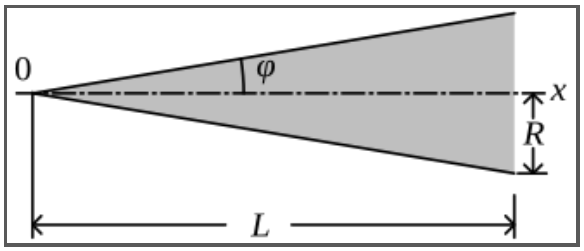

Fig. 1: Geometric profile of conical nose cone

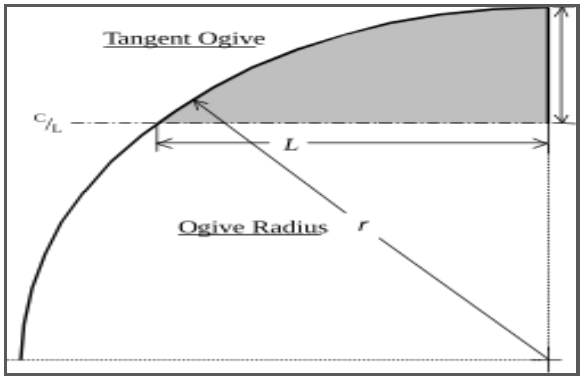

Fig. 2: Geometric profile of tangent ogive nose cone

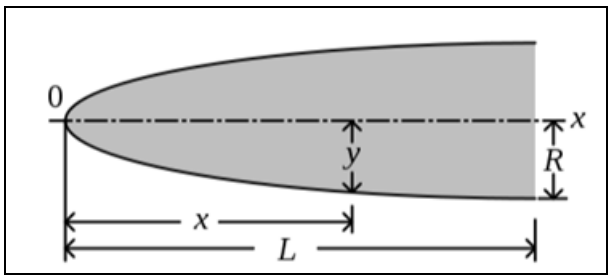

Fig. 3: Geometric profile of parabolic nose cone

B. Computational Setup

The 3D models were imported into ANSYS Workbench 2023 R1. A cylindrical computational domain was created extending 15D upstream, 25D downstream, and 10D radially from the nose axis to ensure undisturbed flow conditions.

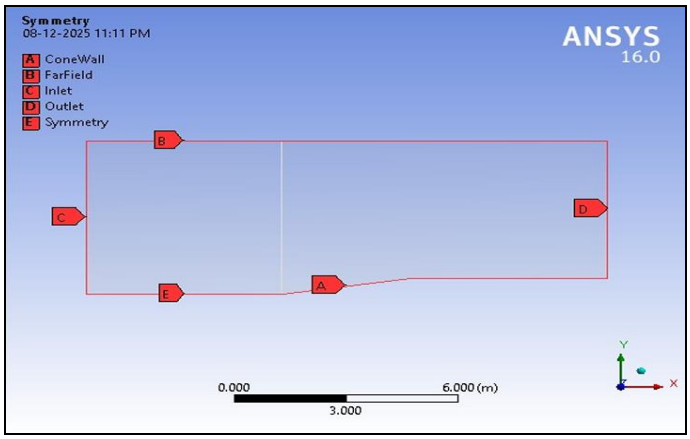

Fig. 4: Computational domain and boundary conditions setup showing far-field boundaries and nose cone placement.

C. Mesh Generation and Independence Study

Unstructured tetrahedral meshes with prismatic boundary layers were generated using ANSYS Meshing. A mesh independence study was conducted for the conical nose (L/D=3.5) to ensure solution accuracy. Three mesh densities were evaluated:

Table 1: Mesh Independence Study Results

Element Size (m)	Number of Elements	Drag Force (N)	% Change
0.10	7,054	1.7371×10^5	-
0.05	27,789	1.7382×10^5	0.06%
0.04	43,335	1.7384×10^5	0.01%

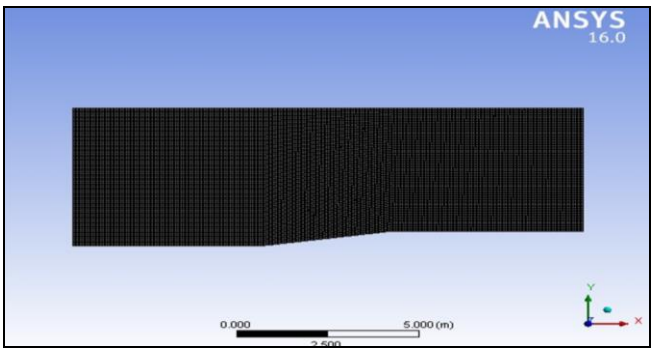

Fig. 5: Computational mesh overall domain

International Journal of Engineering Research & Technology (IJERT)
ISSN: 2278-0181
Vol. 14 Issue 12 , December - 2025

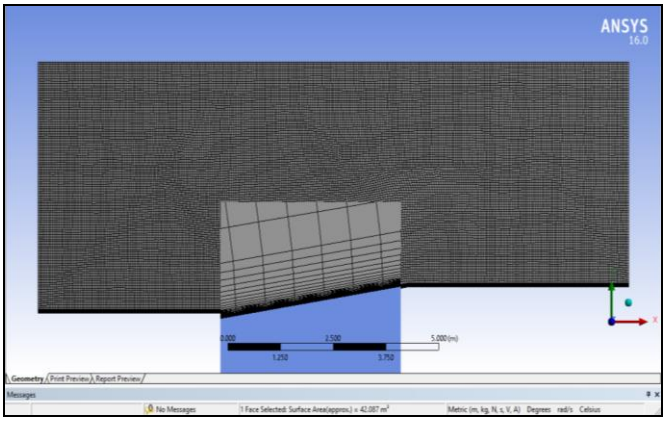

Fig. 6: Computational mesh boundary layer inflation and refined region near nose tip

D. Solver Settings and Boundary Conditions

ANSYS Fluent's pressure-based coupled solver was used with these settings:

- Fluid: Air as ideal gas ($\gamma = 1.4$)
- Inlet: Pressure-far-field, M=3, P=101325 Pa, T=300 K
- Outlet: Pressure-outlet
- Walls: No-slip, adiabatic
- Convergence criteria: Residuals < 10^{-6}

III. RESULTS AND DISCUSSION

A. Flow Field Visualization

Pressure contours revealed distinct shock wave patterns for each geometry. Conical noses produced strong oblique shocks with high pressure concentration at the tip. Tangent ogives showed smoother pressure transitions, while parabolic shapes exhibited the most gradual pressure distributions.

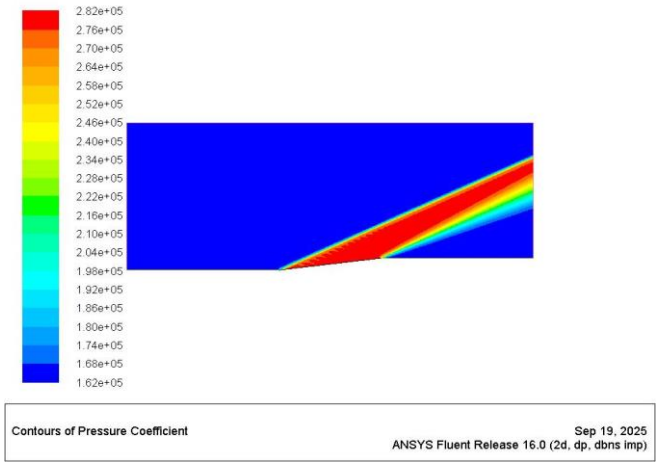

Fig. 7: Pressure contours for of Conical L/D=4.5 showing high pressure concentration

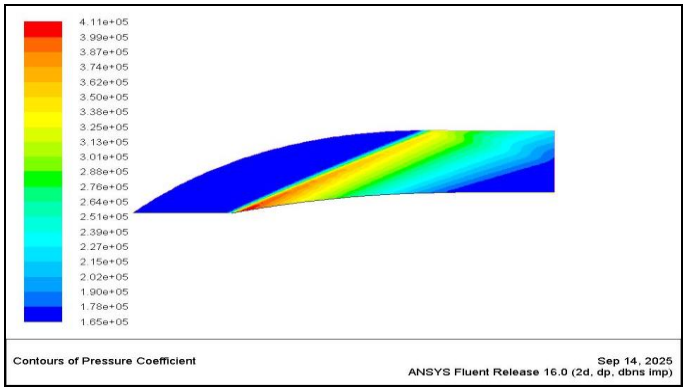

Fig. 8: Pressure contours of Parabolic L/D=4.5 showing smooth pressure distribution.

Mach number distributions confirmed these observations, with conical noses generating the strongest shocks and parabolic noses producing the weakest shock structures. Increasing fineness ratio reduced shock strength for all shapes by allowing the shock to detach further from the body.

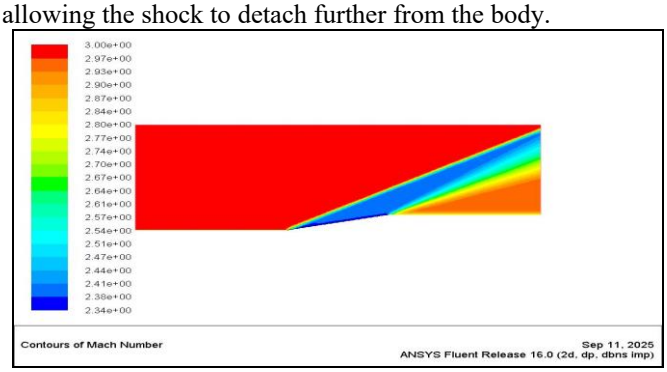

Fig. 9: Mach number distribution of Conical L/D=2.5 showing shock wave patterns.

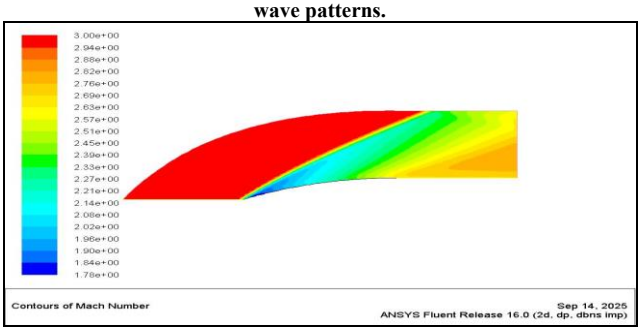

Fig. 10: Mach number distribution of Tangent Ogive L/D=2.5 showing shock wave patterns.

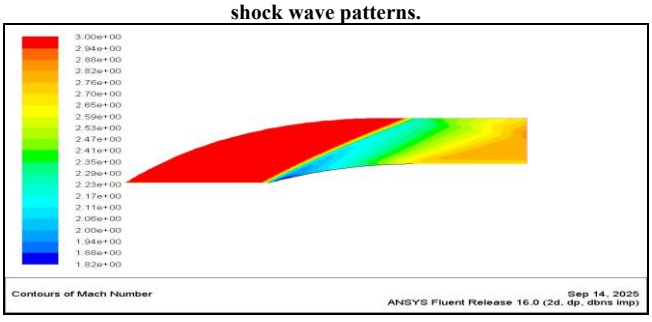

Fig. 11: Mach number distribution of Parabolic L/D=2.5 showing shock wave patterns.

International Journal of Engineering Research & Technology (IJERT)
ISSN: 2278-0181
Vol. 14 Issue 12 , December - 2025

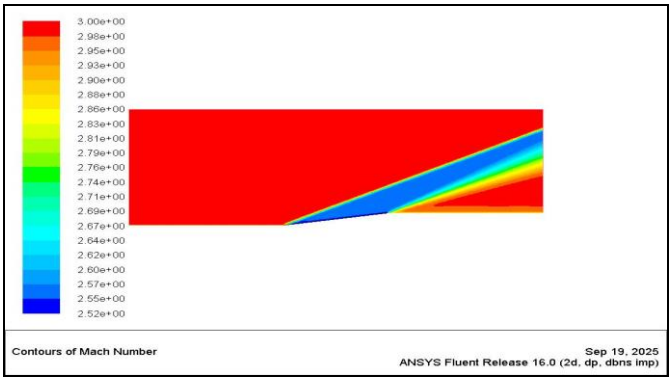

Fig. 12: Shock wave visualization for L/D=3.5 showing shock angle and detachment distance for Conical nose

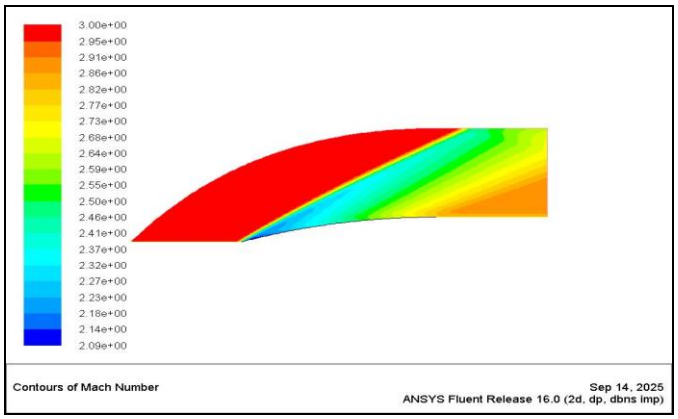

Fig. 13: Shock wave visualization for L/D=3.5 showing shock angle and detachment distance for Tangent Ogive nose

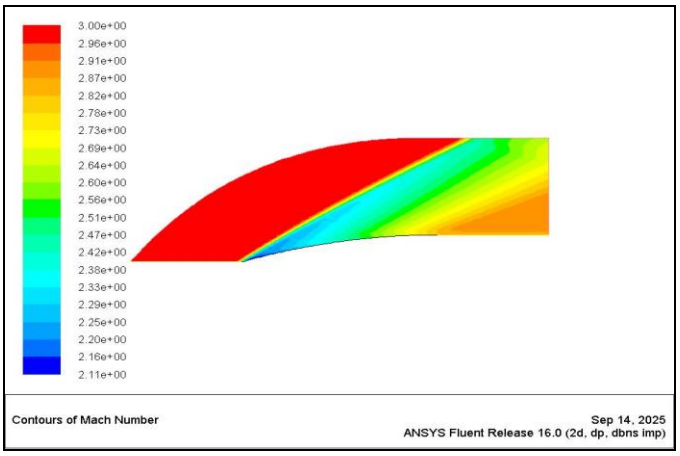

Fig. 14: Shock wave visualization for L/D=3.5 showing shock angle and detachment distance for Parabolic nose

B. Drag Coefficient Analysis

The drag coefficient (Cd) was calculated using:

$$C_d = \frac{D}{0.5 \cdot \rho_\infty \cdot V_\infty^2 \cdot A}$$

where: D = drag force, ρ_∞ = 1.176 kg/m³, V_∞ = 1041.6 m/s, A = 0.950 m².

Table 2: Drag Coefficients for All Configurations

Shape / (L/D)	1.5	2.5	3.5	4.5
Conical	0.586	0.371	0.297	0.251
Tangent Ogive	0.879	0.491	0.365	0.297
Parabolic	0.815	0.361	0.305	0.296

The data reveals several important trends:

1. **Fineness Ratio Dominance**: Increasing L/D consistently reduces drag for all shapes. The improvement from L/D=1.5 to 4.5 is 57% for conical, 66% for tangent ogive, and 64% for parabolic noses.

2. **Shape Performance**: At short lengths (L/D=1.5), conical noses have the lowest drag. At moderate lengths (L/D=2.5), parabolic shapes perform best. At maximum length (L/D=4.5), conical noses achieve the absolute minimum drag (Cd=0.251).

3. **Diminishing Returns**: Drag reduction becomes marginal beyond L/D=3.5, suggesting an optimal range of 3.0-4.0 for practical design.

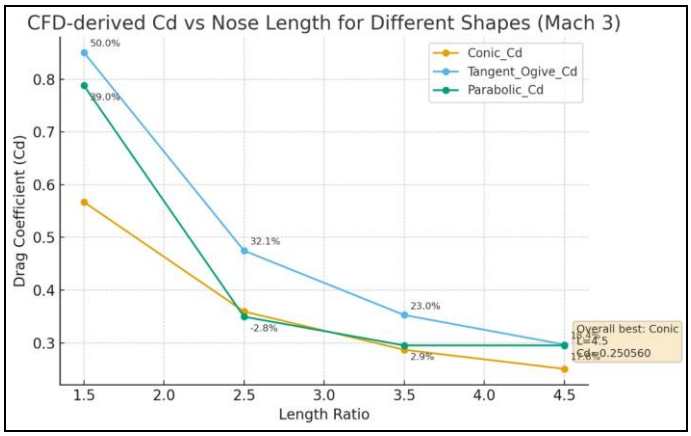

Chart 1: Drag coefficient (Cd) vs. fineness ratio (L/D) showing comparative performance of conical, tangent ogive, and parabolic nose cones at Mach 3.

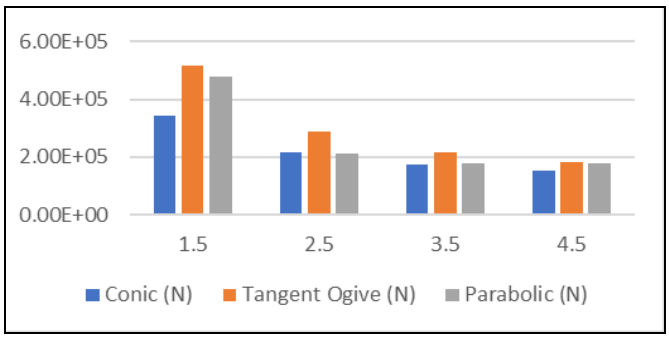

Chart 2: Percentage drag reduction from L/D=1.5 baseline for each shape at different fineness ratios.

International Journal of Engineering Research & Technology (IJERT)
ISSN: 2278-0181
Vol. 14 Issue 12 , December - 2025

C. Surface Pressure Distribution

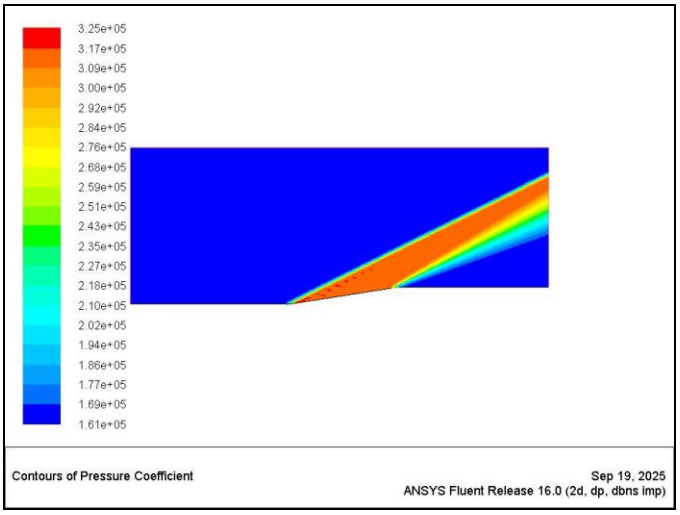

Fig. 15: Fig. 7: Surface pressure distribution along nose cone length for Conical shape at L/D=3.5.

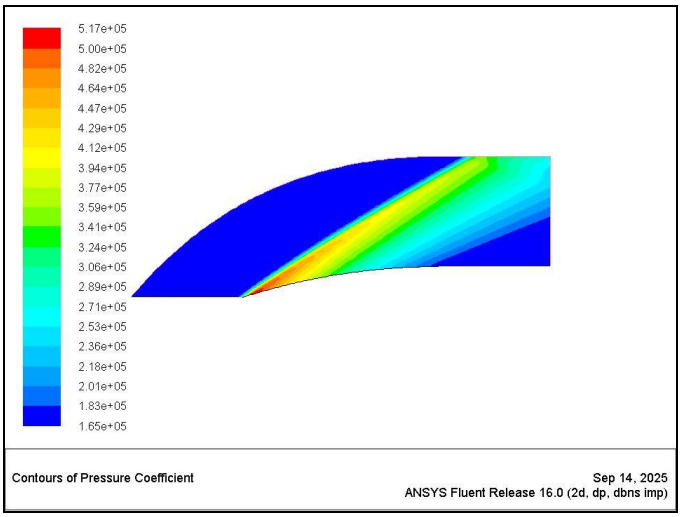

Fig. 16: Surface pressure distribution along nose cone length for Tangent Ogive shape at L/D=3.5.

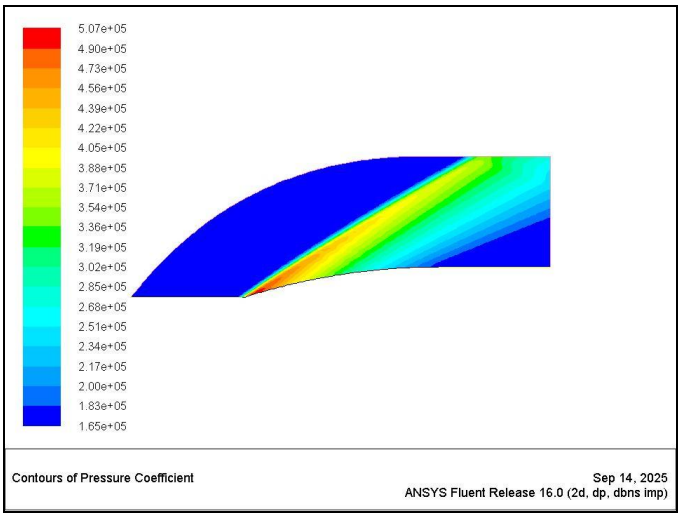

Fig. 17: Surface pressure distribution along nose cone length for Parabolic shape at L/D=3.5.

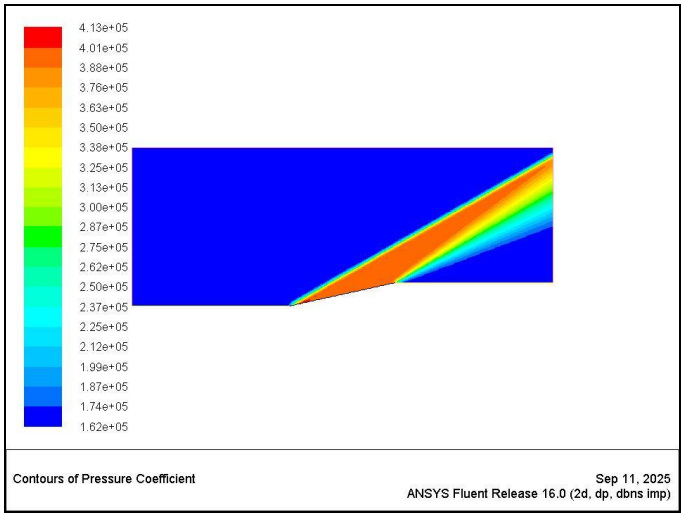

Fig. 18: Pressure coefficient (Cp) comparison at selected axial stations for Conical nose at L/D=2.5.

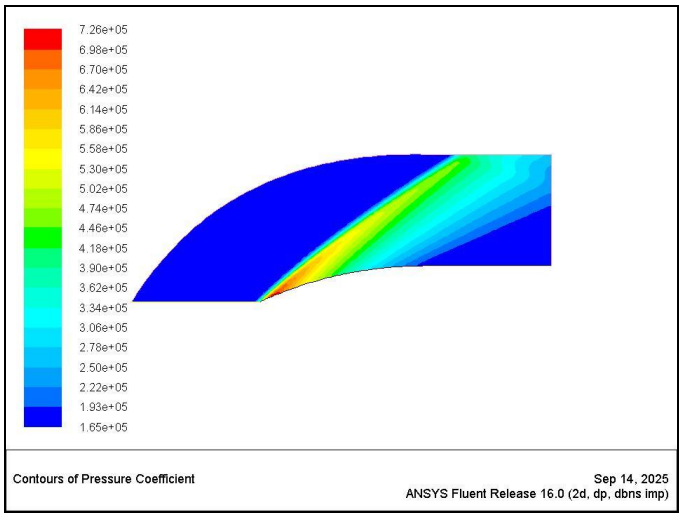

Fig. 19: Pressure coefficient (Cp) comparison at selected axial stations forTangent Ogive at L/D=2.5.

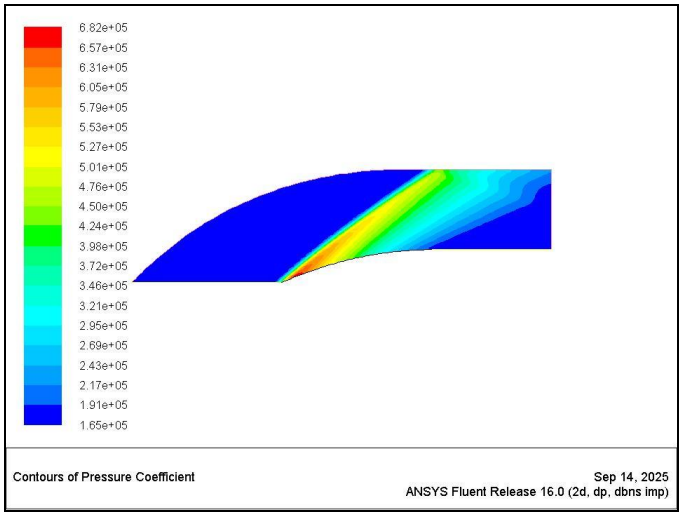

Fig. 20: Pressure coefficient (Cp) comparison at selected axial stations for Parabolic nose at L/D=2.5.

International Journal of Engineering Research & Technology (IJERT)
ISSN: 2278-0181
Vol. 14 Issue 12 , December - 2025

D. Comparison with Theoretical Predictions

The results align with classical oblique shock theory. The θ-β-M relation predicts that smaller flow deflection angles (achieved through higher fineness ratios) produce weaker shocks with lower drag. For the conical nose with L/D=4.5 (θ=6.3°), the theoretical shock angle is 21.0°, closely matching the CFD-extracted value of 20.6° (error: 1.9%).

Table 3: CFD-predicted θ-β-Mach values for conical nose cones at Mach 3.

Cone Half-Angle (θ ≈ α)	Mach (M_1)	Shock Angle (β)
18.4°	3.0	≈ 36.5°
11.3°	3.0	≈ 27.0°
8.1°	3.0	≈ 23.0°
6.3°	3.0	≈ 21.0°

IV. CONCLUSION

This CFD study successfully analyzed and compared the aerodynamic performance of three nose cone geometries at Mach 3. The key findings are:

1. Fineness ratio (L/D) is the dominant parameter for drag reduction in supersonic flight, with increasing slenderness consistently lowering drag coefficients across all shapes.
2. The conical nose cone with L/D=4.5 achieved the lowest drag (Cd=0.251), demonstrating that simple geometries can outperform complex curved profiles at high fineness ratios.
3. The parabolic shape offers excellent performance at moderate lengths (L/D=2.5, Cd=0.361), providing a balanced design compromise.
4. Practical design should target fineness ratios in the range of 3.0-4.0, where aerodynamic benefits are significant without excessive structural penalties.

For maximum performance applications where drag minimization is critical, the conical nose with L/D=4.5 is recommended. For general supersonic aircraft requiring balanced performance, the parabolic nose with L/D=2.5-3.5 is optimal.

V. FUTURE WORK

Future studies could extend this analysis to different Mach numbers (2, 4, 5), incorporate aerodynamic heating effects, include structural optimization, and validate results through wind tunnel testing. Advanced optimization techniques like genetic algorithms could further refine nose cone shapes.

ACKNOWLEDGMENTS

The authors thank Malla Reddy College of Engineering & Technology for providing computational resources and ANSYS software access. We acknowledge the guidance of department faculty members throughout this research project.

REFERENCES

[1] J.D. Anderson, "Fundamentals of Aerodynamics", 6th edition, McGraw-Hill, 2017.
[2] J.J. Bertin and R.M. Cummings, "Aerodynamics for Engineers", 6th edition, Pearson, 2014.
[3] S.Z. Pinier and W.L. Hankey, "Aerodynamic Performance of Various Nose Cone Shapes at Supersonic Speeds", Journal of Spacecraft and Rockets, vol. 22, no. 3, 1985.
[4] E.S. Love, "Aerodynamic Problems of Manned Space Vehicles", Journal of the Aeronautical Sciences, vol. 26, no. 2, 1959.
[5] V. Kumar and R.K. Singh, "CFD Analysis of Different Nose Cone Shapes at Supersonic Speed", International Journal of Engineering Research and Applications, vol. 3, no. 4, 2013.
[6] M.P. Netterfield, "Pressure and Force Characteristics of Tangent Ogive Nose Cylinders at Mach Numbers from 2.5 to 4.5", DSTO-TR-0482, 1997.
[7] F.R. Menter, "Two-Equation Eddy-Viscosity Turbulence Models for Engineering Applications", AIAA Journal, vol. 32, no. 8, 1994.
[8] H.K. Versteeg and W. Malalasekera, "An Introduction to Computational Fluid Dynamics: The Finite Volume Method", 2nd edition, Pearson, 2007.
[9] ANSYS Inc., "ANSYS Fluent User's Guide", Release 2023 R1, 2023.
[10] J.D. Anderson, "Modern Compressible Flow: With Historical Perspective", 4th edition, McGraw-Hill, 2021.